MULTI-WAVELENGTH STUDY OF NEW 95 GHz METHANOL MASERS

Vwavware, O J. Chima A.I .and Ojobeagu, O A

[1,2,3] **Department of Industrial Physics, Enugu State University of Science and Technology.**

Correspondence author's email: abraham.chima@esut.edu.ng

ABSTRACT

A multi-wavelength study has been conducted on the 95 GHz methanol maser source G010.3203-00.2589 with its BGPS counterpart G010.320-00.258. We have used data from GLIMPSE (3.6, 4.5, 5.8, 8.0 μm), MIPSGAL (24 μm), Hi-GAL (70, 160, 250, 350, 500 μm), ATLASGAL (870 μm) and BGPS (1.1 mm) catalogues to perform a spectral energy distribution analysis of 95 GHz methanol maser. The spectral energy distribution of the peak flux against wavelength reveals a skewed normal distribution with a correlation coefficient of -0.12967953 (-12.96%). From the analysis and Gaussian fitting, the source peaked at near-infrared 160 μm Hi-GAL waveband. We obtained a source temperature of 18.125 K and the source luminosity as 5.752×10^{18}W which is equivalent to 1.5026×10^{-8} $L_{\odot}$. This indicates that the source is still at infant stage compared to our Sun.

INTRODUCTION

Methanol masers are very common in star forming regions and they are widespread in our Galaxy, with more than 20 transitions in a wide frequency range, from centimetre to millimetre, discovered to date (Cragg *et al.*, 2005). Their observed connections with other star formation activities (e.g Infrared dark clouds, millimetre and submillimetre dust continuum emissions and ultracompact (UC) HII regions) has made them one of the most effective tools for investigating star forming region (Ellingsen 2006). The trigonometric parallaxes of methanol maser provide a direct and accurate measurement of distances to the star formation regions wherein they reside (Xu *et al.*, 2006; Rygl *et al.*, 2010). Their multiple frequency transitions enable us to investigate the physical and chemical conditions of star forming regions (Leurini *et al.*, 2007; Purecell *et al.*, 2009) and evolutionary stages of star formation.

According to empirical classification, methanol masers can be divided into two classes (class I and II) depending on their exciting locations (Batrla 1988 and Menten 1991). Class I methanol masers are usually found offset from the presumed origin of excitation, and can be further expanded to include widespread Class I methanol maser (e.g 44 and 95 GHz) and a rare or weak Class I methanol masers (e.g 9.9 and 104 GHz, Voronkov *et al.*, 2012). Rare or weak methanol masers trace stronger shock regions, which have higher temperature and densities with regard to widespread masers (Sobolev *et al.*, 2005; Voronkov *et al.*, 2012). In contrast, Class II methanol masers are often found to reside close to high mass stellar objects (Caswell *et al.*, 2010) and are frequently associated with UC HII regions, infrared sources, and OH masers.

The process of formation of high mass stars with masses roughly eight times that of the Sun, or more, remains a big challenge to modern astronomy. High mass stars are vital for study because of their ability to inject matter and energy into the interstellar medium of galaxies throughout their lifetimes. Observing high mass star formation is difficult, though, because massive star

forming regions are farther away than their low mass counterparts. High mass stars form in clusters and begin the process of nuclear fusion even as they are accreting matter. One of the key issues is whether their formation is a scaled-up version of the low mass star formation process, complete with disk and outflows, or whether high mass stars form by coalescence of low mass stars. Being compact and bright sources, masers offer a unique opportunity to peer into the deep interior of high mass star forming regions at high angular resolution. In this work, we use data on the 95 GHz methanol maser from the data base catalogue, along with other associated star formation tracers, to gain insight into the high mass star formation process by investigating their flux variation at different wavelength in order to construct a spectral energy distribution that will be used to provide specific parameters about these sources/regions.

Materials

This research was done using existing data on 95 GHz Class I methanol masers. Since Class I methanol masers generally occur in outflows, we began by looking for high angular resolution data on Class I methanol masers in star forming regions. Val'tts and Larionov (2007) compiled a catalogue of all the known Class I methanol masers. Chen *et al.* (2012) mapped 214 sources for search of 95 GHz methanol maser. From their observations, about 63 sources exhibited 95 GHz methanol maser capabilities.

Methods

We examined the relationship between the peak flux densities of the sixty-three 95GHz methanol masers whose data are provided in the Appendix C to their velocities. Spectral analysis and visualization of data where done using the python programming software. A number of python packages such as numpy, matplotlib, pandas, scipy and astropy were used in constructing the SED and fittings.

We plotted the fluxes of the 63 sources to their wavelengths. From the distribution, we identified the source G010.3203-00.2589 corresponding to the greatest flux density. Furthermore, we searched for the peak flux density of G010.3203-00.2589 using GLIMPSE, MIPSGAL, Hi-GAL, ATLASGAL and BGPS catalogues in VizieR. The obtained data from these catalogues and their matching wavelengths were used visualizing a spectral energy distribution of the source.

RESULTS AND DISCUSSIONS

Data Analysis and results

We begin by examining the relationship between the Peak flux densities of the sixty-three 95GHz methanol masers to their centre velocities. Figure 1.1 is a visualization of the scatter plot of the peak flux densities to their centre velocities. From the Figure 1.1, it can be seen that more fluxes are concentrated from 20 km/s to 100 km/s and that these fluxes lie mainly from 1 to 10 Jy. About 3 sources are seen to peak above 20 Jy.

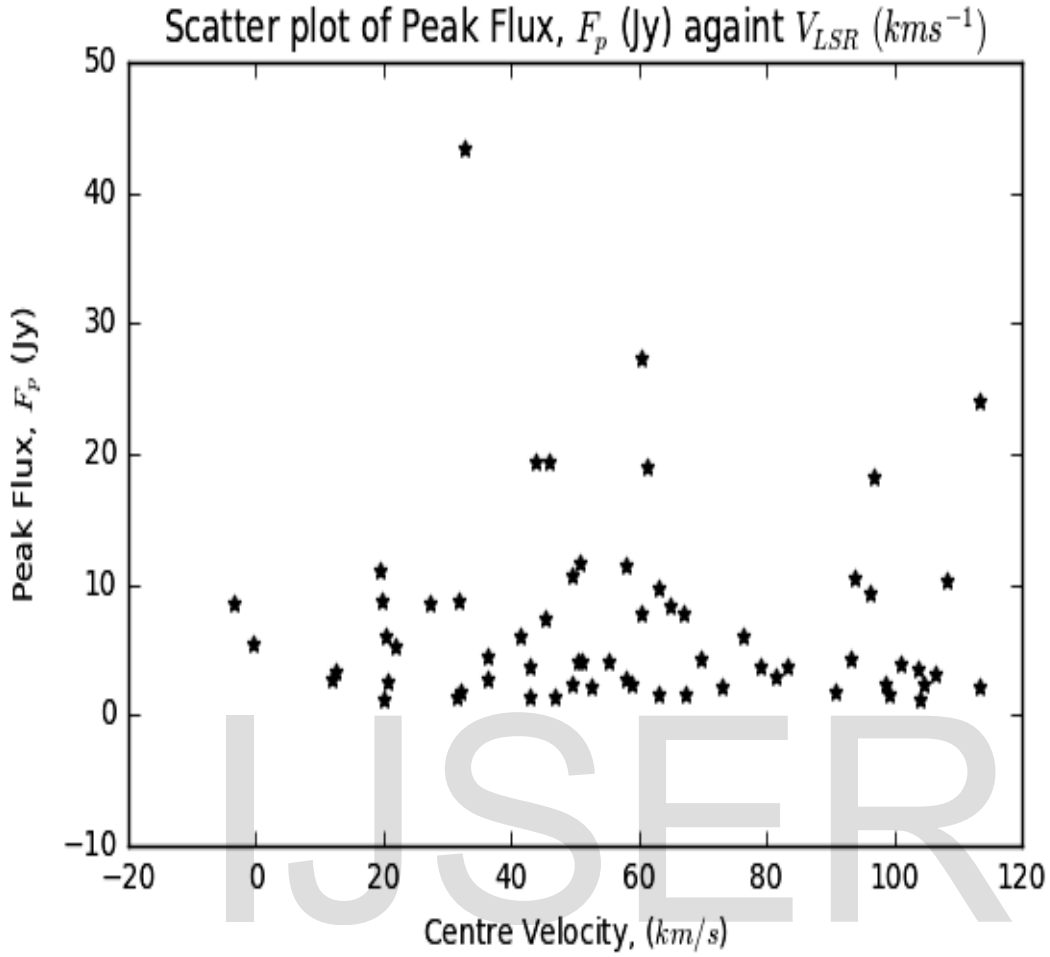

Figure 1.1: Scatter plot of Peak flux densities against centre velocities

The histogram of the centre velocity is shown in Figure 1.2. The diagram reveals a slightly normal distribution except for a bi-modal shape witnessed at 60 km/s and 100 km/s^{-1}.

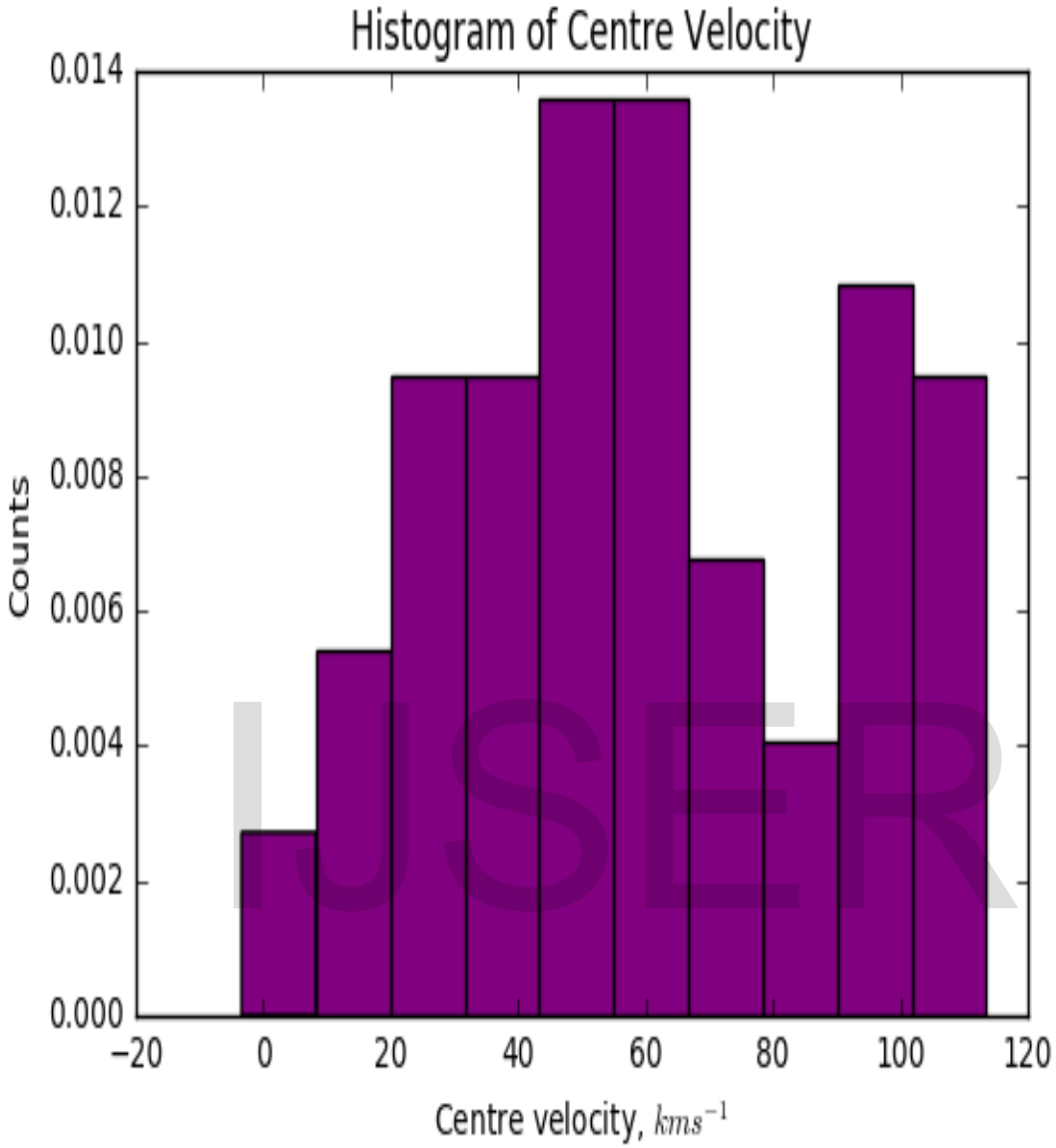

Figure 1.2: Histogram of the Centre velocity of the 63 95 GHz Methanol Masers.

A scatter plot of Source Luminosity and Gas mass of the 95 GHz Methanol masers is shown in Figure 1.3. Majority of the sixty-three 95GHz Methanol masers exhibit masses ranging from 0 to 10,000 $M_{\odot}$ whereas others are sparsely distributed.

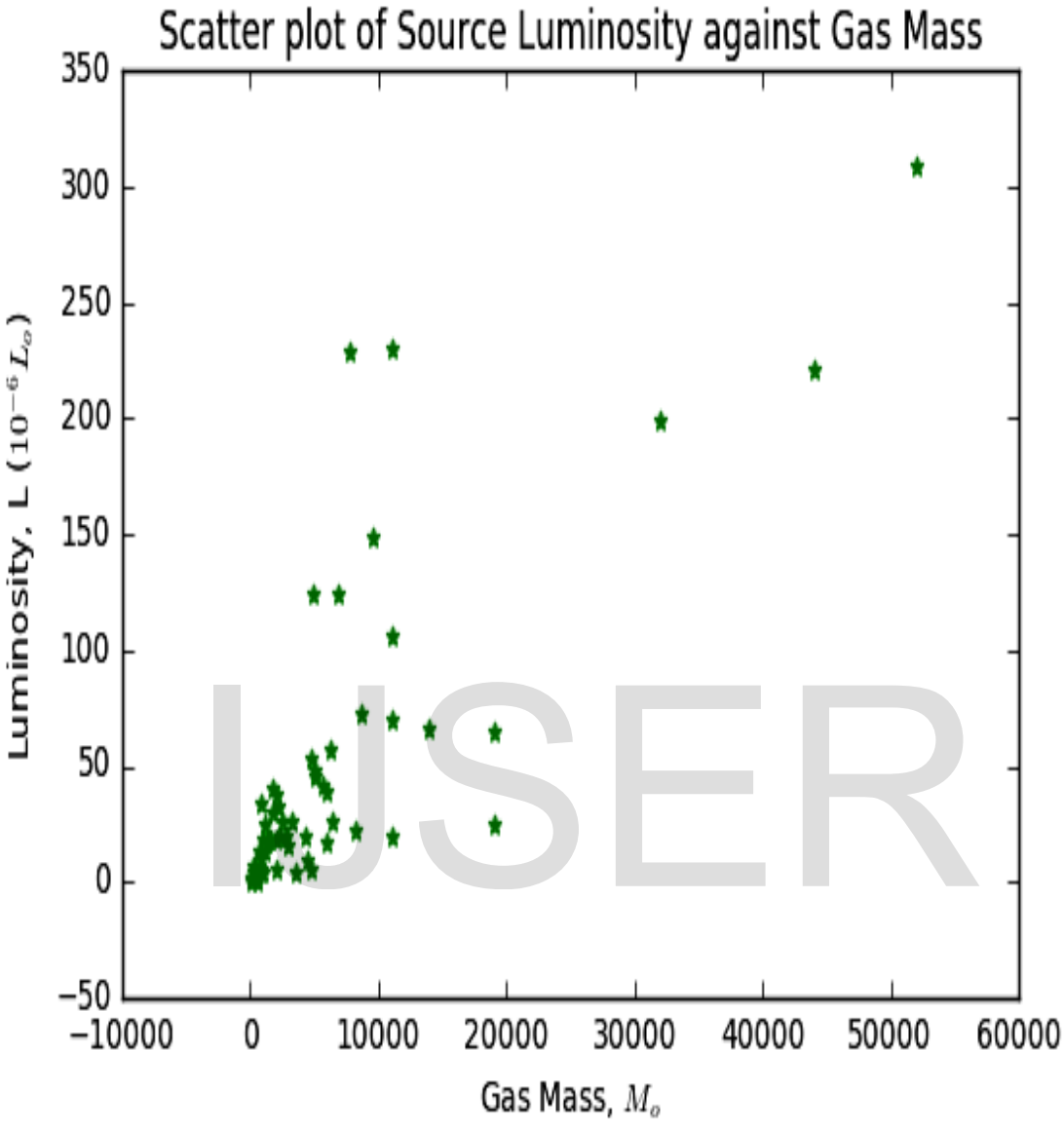

Figure 1.3: Scatter plot of Luminosity against Gas Mass

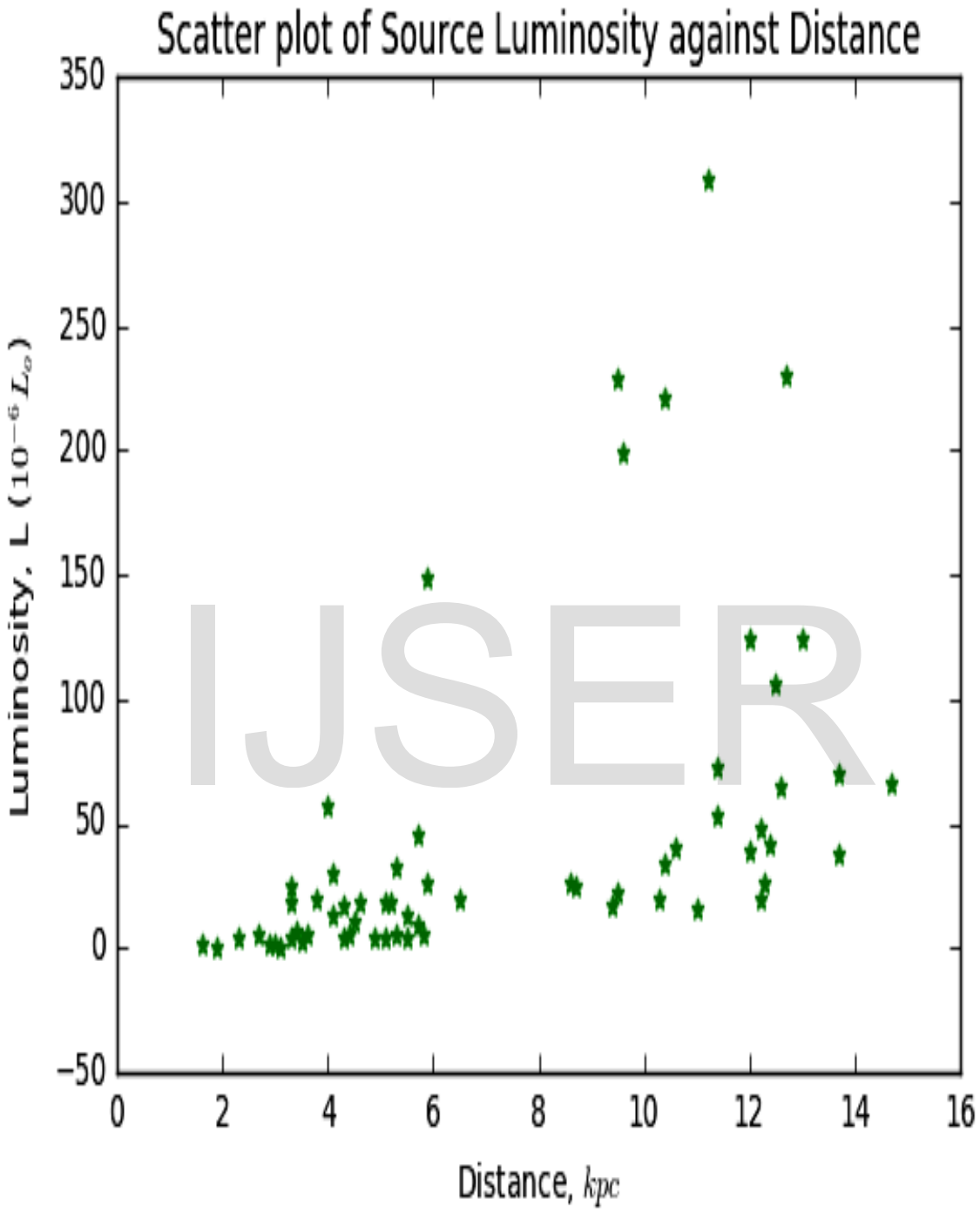

Figure 1.4: Scatter plot of Source luminosity against distances

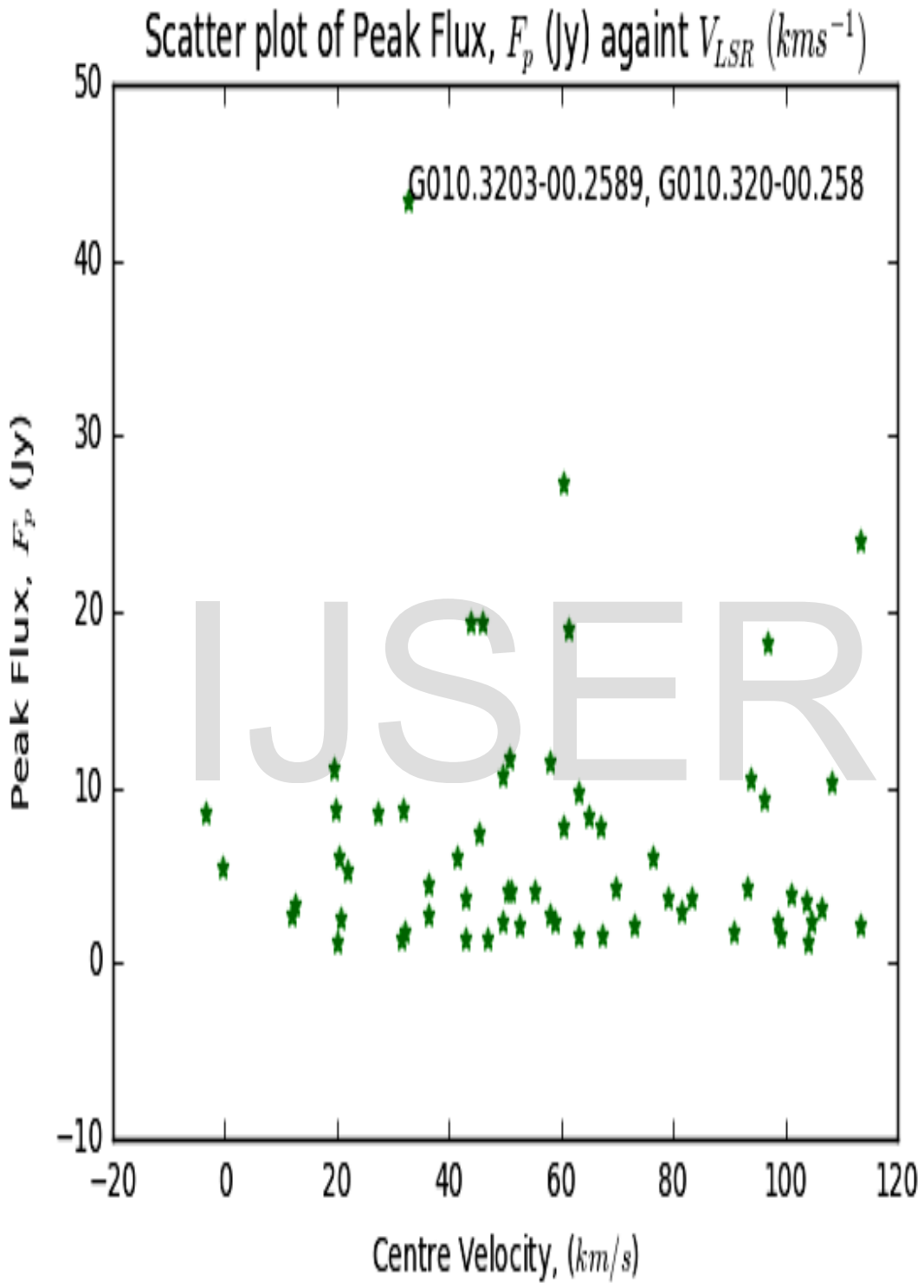

Figure 1.5: Scatter plot of Peak flux densities against centre velocities showing the source with greater peak flux.

A closer look at the scatter plot of the peak flux against centre velocity (Fig. 1.5) reveals that the source with the highest peak flux is G010.3203-00.2589 (BGPS Name: G010.320-00.258). This source shall be our source of interest since it has a greater peak flux.
Therefore, we selected the maser source G010.3203-00.2589with coordinates (Right Ascension = 18 9 23.13 and Declination = -20 8 8.7) and its counterpart BGPSG010.320-00.258from (Xi Chen *et al*., 2012). We searched for this source in many catalogues in order to find its flux density as well as its associated wavelengths. Searches were made with the following catalogues: GLIMPSE (3.6, 4.5, 5.8 and 8.0 μmIRAC Bands), MIPSGAL (24μm), Hi-GAL (70, 160, 250, 350, 500μm), ATLASGAL (870 μm) and finally the BGPS (1.1 mm). We also ensure that the search radius of the source did not exceed 1 arc-minute radius so as to ensure that the information gotten matches or lies within the maser core region. Table 1.1 contains the flux property of the source at different wavelengths.

Table 1.1: Flux density property of BGPSG010.320-00.258 at GLIMPSE, MIPSGAL, Hi-GAL, ATLASGAL and BGPS wavelengths

Wavelength (μm)	Flux(mJy)	Flux-uncertainty(mJy)
3.6	7.630	0.874
4.5	51.900	5.390
5.8	147.000	12.300
8.0	255.000	69.500
24.0	111.509	4.920
70.0	1.84000.000	534.000
160.0	298000.000	1180.000
250.0	249000.000	1480.000
350.0	116000.000	1420.000
500.0	49200.000	1740.000
870.0	2390.000	370.000
1100.0	3360.000	270.000

Analysis and Results of G010.3203-00.2589

We begin our analysis with the visualization of the plot of the Flux (mJy) against the wavelength in μm in order to obtain the Spectral energy distribution (SED) of the 95 GHz methanol maser source G010.3203-00.2589 with coordinates: Right Ascension 18 9 23.13 and Declination -20 8 8.7 and its counterpart source BGPS G010.320-00.258. The spectral energy distribution is shown in Figure 1.6 and 1.7.

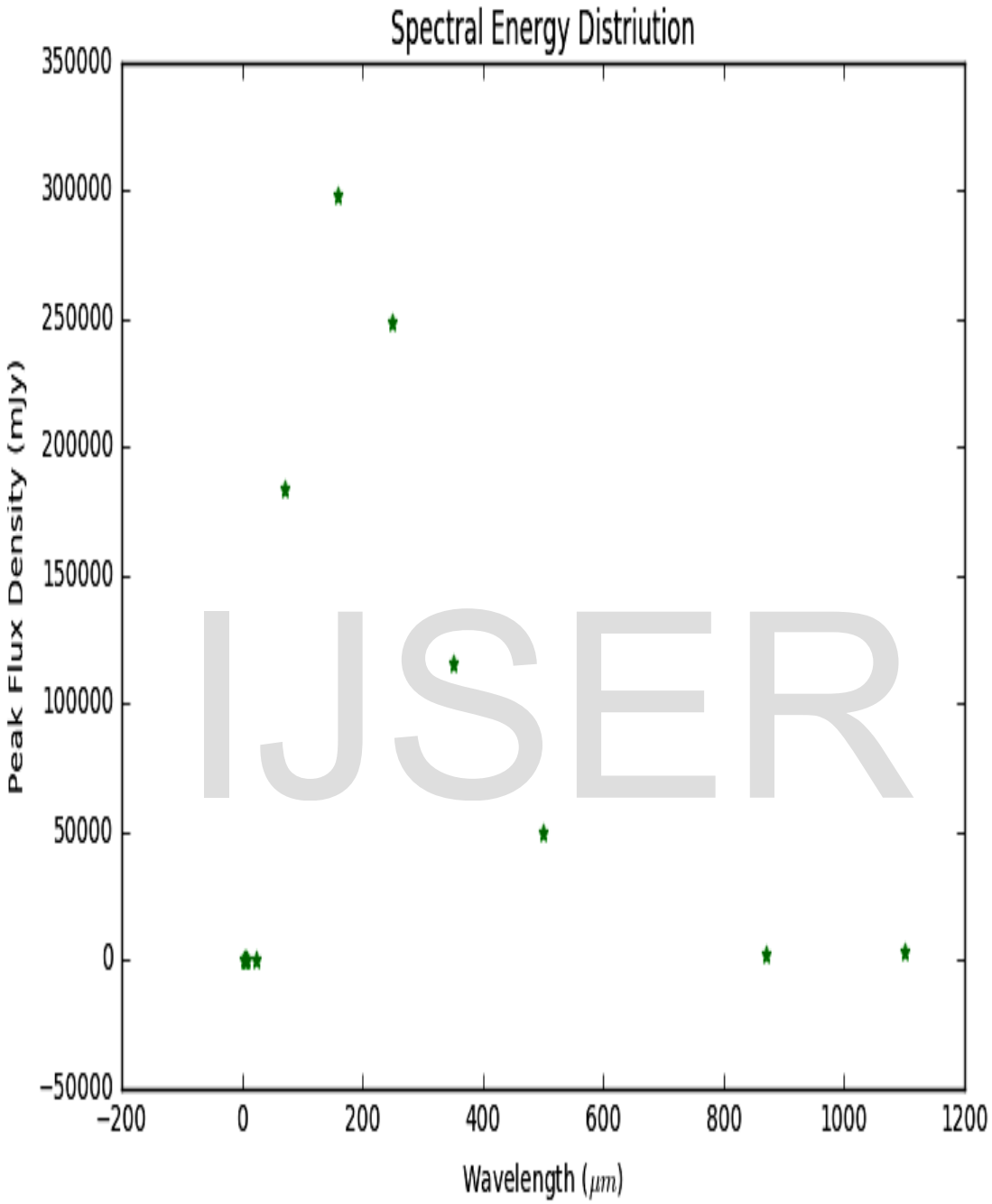

Figure 1.6: Scatter plot of the Spectral Energy Distribution of Maser source G010.3203-00.2589.

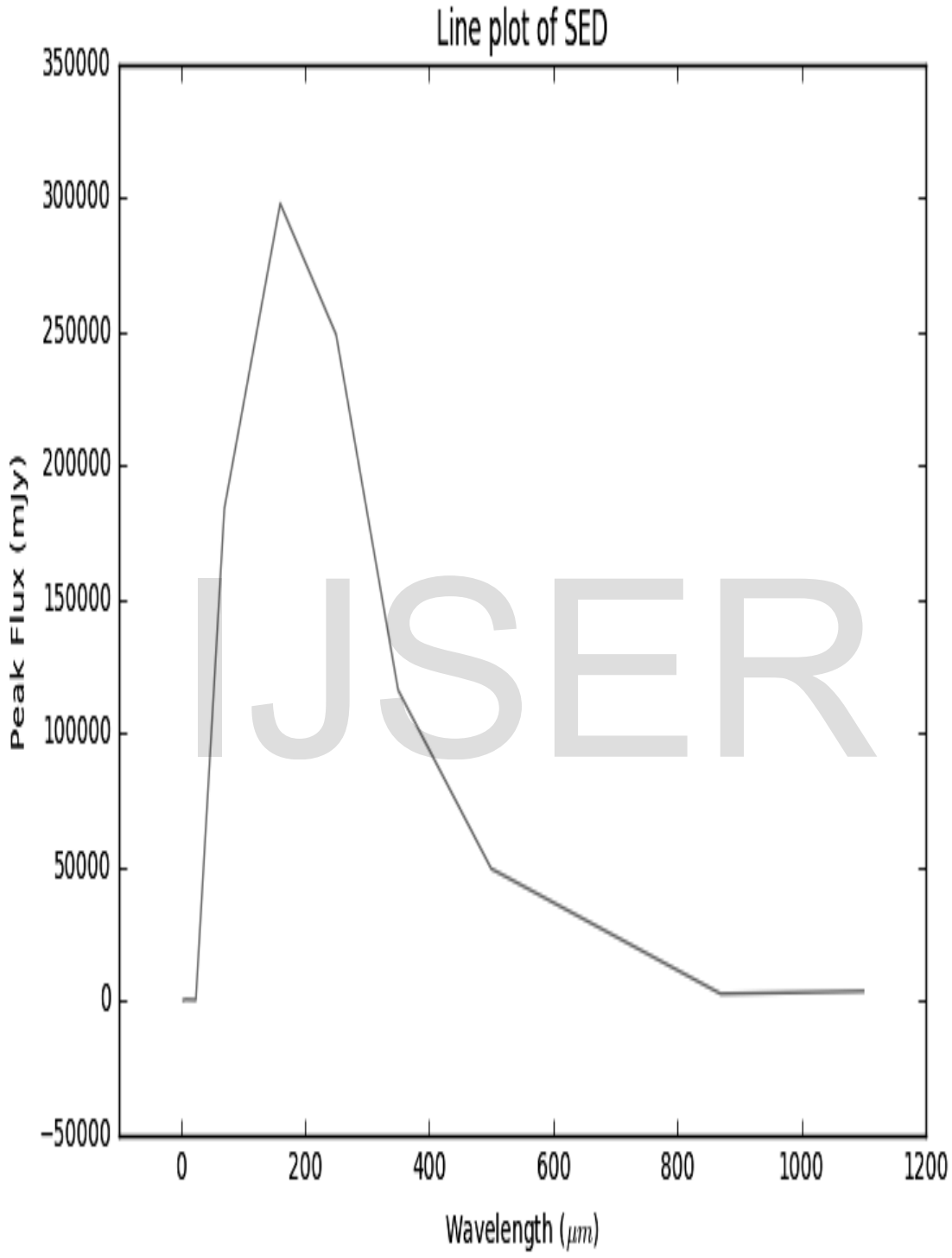

Figure 1.7: Line plot of the Spectral Energy Distribution of Maser source G010.3203-00.2589.
Figure 1.6 shows the scatter plot of the SED of the source while Figure 1.7 shows the line-curve of the source. From both figures, it can be seen that the curve follows a normal distribution

except that it is slightly skewed to the left. This could be as a result of the inadequate data available for the source as the correlation coefficient indicates a value of -0.12967953 (-12.96%).Figure 1.8 shows the Gaussian fit applied on the SED in order to normalize it.

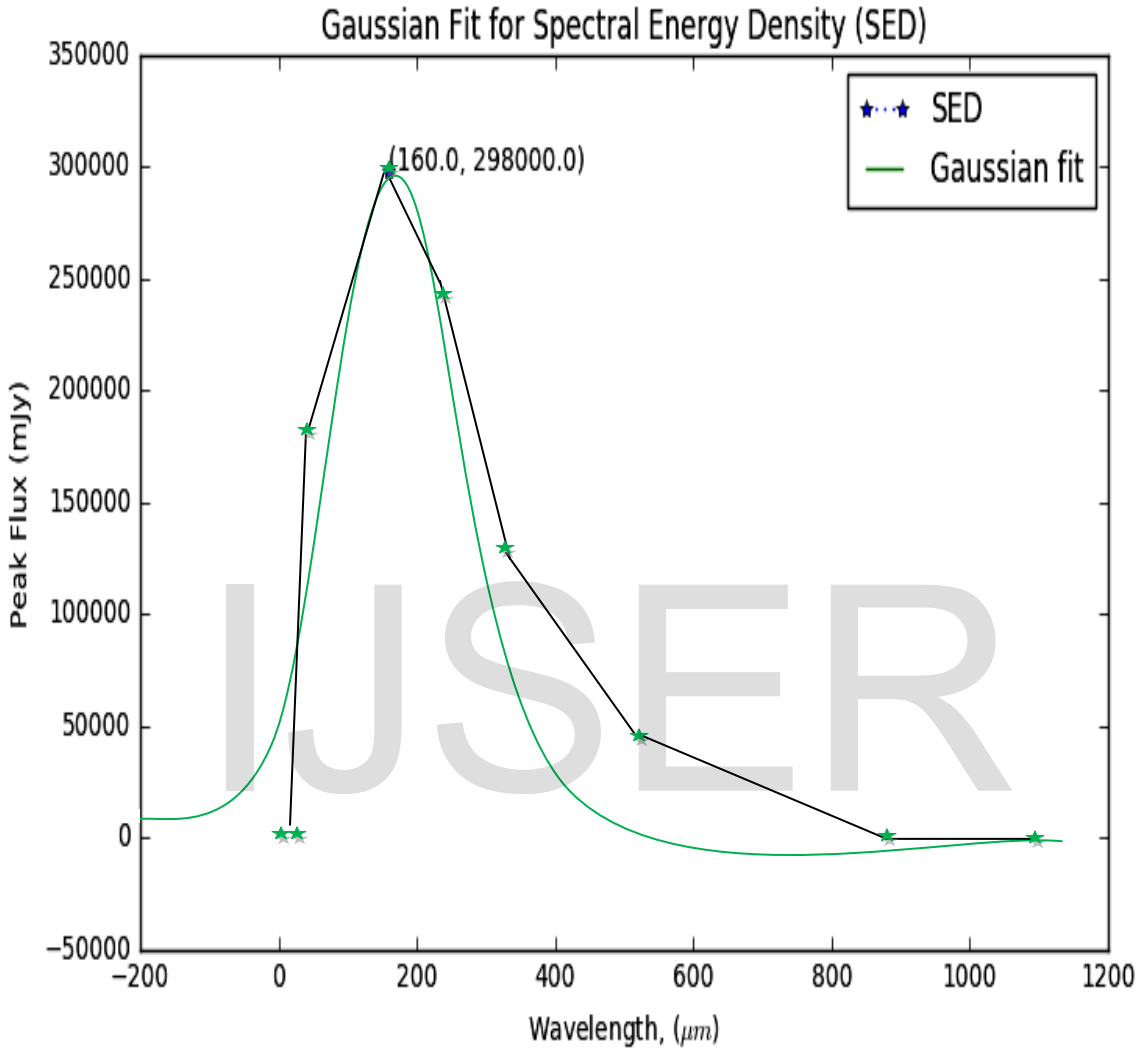

Figure 1.8: Gaussian fit of the Spectral Energy Distribution of Maser source G010.3203-00.2589.

Discussion

We plotted the fluxes of the 63 sources to their wavelengths. From the distribution, we identified the source G010.3203-00.2589 corresponding to the greatest flux density. Furthermore, we searched for the peak flux density of G010.3203-00.2589 using the GLIMPSE, MIPSGAL-GAL, ATLASGAL and BGPS catalogues in VizieR. The obtained data from these catalogues and their matching wavelengths were used in visualising a spectral energy distribution of the source.

From our analysis (Fig.1.8), we were able to identify the peak flux and its associated wavelength. The SED flux peaked at 298000 mJy (298Jy) and its equivalent wavelength, λ_{max} at 160 μm (this falls within the Hi-GAL survey wavelength).

Using the Wien's displacement law, $\lambda_{\max} = \frac{b}{T}$ where $b = 2.897 \times 10^{-3}$, we obtain a source temperature of 18.125 K. Also, we compute the luminosity of the source using the relation $L = 4\pi d^2 P$ and we obtained the luminosity, L as 5.752×10^{18}Wwhich is equivalent to $1.5026\times10^{-8}L_{\odot}$. This indicates that the source is still at infant stage compared to our Sun.

Conclusion

A multi-wavelength study has been conducted on the 95 GHz methanol maser source G010.3203-00.2589 with its BGPS counterpart G010.320-00.258. We have used data from GLIMPSE (3.6, 4.5, 5.8, 8.0 μm), MIPSGAL (24 μm), Hi-GAL (70, 160, 250, 350, 500 μm), ATLASGAL (870 μm) and BGPS (1.1 mm) catalogues to perform a spectral energy distribution analysis of 95 GHz methanol maser.

Spectral analysis and visualization of data were done using the Python programming software. A number of Python packages such as numpy, matplotlib, pandas, scipy and astropy were used in constructing the SED and fittings.

We plotted the fluxes of the 63 sources to their wavelengths. From the distribution, we identified the source G010.3203-00.2589 corresponding to the greatest flux density. Furthermore, we searched for the peak flux density of G010.3203-00.2589 using the GLIMPSE, MIPSGAL, Hi-GAL, ATLASGAL and BGPS catalogues in VizieR. The obtained data from these catalogues and their matching wavelengths were used in visualising a spectral energy distribution of the source.

From our analysis, we obtained a peak flux of 298000 mJy (298 Jy) forG010.3203-00.2589 and a source temperature of 18.125 K. Also, using the luminosity-flux relationship, a luminosity of 5.752×10^{18}W which is equivalent to 1.5026×10^{-8} $L_{\odot}$ was obtained for the source. This indicates that the source is still at infant stage compared to our Sun.

REFERENCES

Barrett, A. H., Martin, R. N., Myers, P. C., & Schwartz, P. R. (1972). Observations of Methanol in Sagittarius b2 at 48 GHSz. *The Astrophysical Journal Letters*, *178*, L23.

Batrla, W., & Menten, K. M. (1988). Detection of a strong new maser line of methanol toward DR 21(OH). *The Astrophysical Journal Letters*, *329*, L117–L120.

Carey, S. J., Noriega-Crespo, A., Mizuno, D. R., Shenoy, S., Paladini, R., Kraemer, K. E., Testi, L. (2009). MIPSGAL: A Survey of the Inner Galactic Plane at 24 and 70 μm. *Publications of the Astronomical Society of the Pacific*, *121*(875), 76.

Chen, X., Ellingsen, S. P., & Shen, Z.-Q. (2009). Class I methanol masers: masers with extended green objects. *Monthly Notices of the Royal Astronomical Society*, *396*(3), 1603–1609.

Chen, Xi, Ellingsen, S. P., He, J.-H., Xu, Y., Gan, C.-G., Shen, Z.-Q., … Ju, B.-G. (2012). A 95 GHz Class I Methanol Maser Survey toward a Sample of GLIMPSE Point Sources Associated with BGPS Clumps. *The Astrophysical Journal Supplement Series*, *200*(1), 5.

Chen, Xi, Ellingsen, S. P., Shen, Z.-Q., Titmarsh, A., & Gan, C.-G. (2011). A 95 GHz Class I Methanol Maser Survey Toward Glimpse Extended Green Objects (EGOs). *The Astrophysical Journal Supplement Series*, *196*(1), 9.

Cragg, D. M., Sobolev, A. M., & Godfrey, P. D. (2005). Models of class II methanol masers based on improved molecular data. *Monthly Notices of the Royal Astronomical Society*, *360*(2), 533–545.

Ellingsen, S. P. (2006). Methanol Masers: Reliable Tracers of the Early Stages of High-Mass Star Formation. *The Astrophysical Journal*, *638*(1), 241.

Menten, K.M. (1991). The Discovery of a New, Very, Strong and Widespread Interstellar Methanol Maser Line. The Astrophysics Journal, 380, L75.

Menten, K. M., Walmsley, C. M., Henkel, C., & Wilson, T. L. (1988). Methanol in the Orion region. I - Millimeter-wave observations. II - The 25 GHz masers revisited. *Astronomy and Astrophysics*, *198*, 253–273.

Rebolledo, D., Wong, T., Leroy, A., Koda, J., & Meyer, J. D. (2012). Giant Molecular Clouds and Star Formation in the Non-grand Design Spiral Galaxy NGC 6946. *The Astrophysical Journal*, *757*(2), 155.

Rosolowsky, E., Dunham, M. K., Ginsburg, A., Bradley, E. T., Aguirre, J., Bally, J., … Williams, J. P. (2010). The Bolocam Galactic Plane Survey -- II. Catalog of the Image Data. *The Astrophysical Journal Supplement Series*, *188*(1), 123–138.

Sobolev, A. M., Ostrovskii, A. B., Kirsanova, M. S., Shelemei, O. V., Voronkov, M. A., & Malyshev, A. V. (2006). Methanol Masers and Star Formation. *ArXiv:Astro-Ph/0601260*.

Val'tts, I. E., & Larionov, G. M. (2007). A general catalog of class I methanol masers. *Astronomy Reports*, *51*(7), 519–530.

Voronkov, M. A., Caswell, J. L., Ellingsen, S. P., Green, J. A., & Breen, S. L. (2014). Southern class I methanol masers at 36 and 44 GHz. *Monthly Notices of the Royal Astronomical Society*, *439*(3), 2584–2617.

Yang, W., Xu, Y., Chen, X., Ellingsen, S. P., Lu, D., Ju, B., & Li, Y. (2017). A New 95 GHz Methanol Maser Catalog. I. Data. *The Astrophysical Journal Supplement Series*, *231*(2), 20.